

# Microstructure and selected properties of Ni-Cr-Re coatings deposited by means of HVOF thermal spraying

## Abstract

The article presents selected results of testing Ni-Cr-Re coatings deposited by means of HVOF supersonic spray. The substrate made of 16Mo3 chromium molybdenum boiler steel was sprayed with a powder material of Oerlikon Amdry 4535 80% Ni, 20% Cr, 20÷45 µm, to which 1% of metallic rhenium was added using the high energy milling method in a ball mill. The Rhenium is an alloying additive that improves the heat resistance of alloys, creep and high temperature oxidation resistance. Alloys with the addition of rhenium are widely used in the aerospace industry (nickel superalloys) and in power industry. Metallographic microscopic examinations, microhardness tests and surface profilometry were carried out.

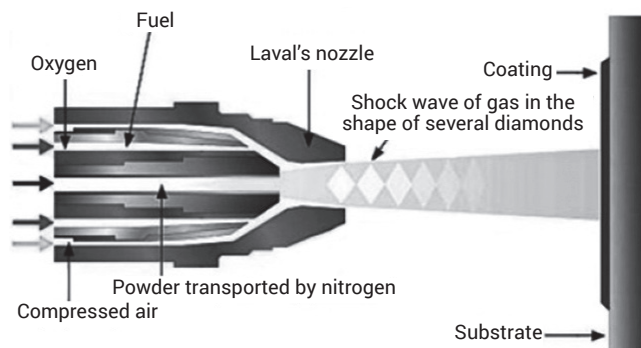
### Keywords:

HVOF spraying process;  
coatings;  
thermal spraying

## Introduction

HVOF (High Velocity Oxy Fuel) supersonic flame spraying consists of bombarding the substrate with a stream of coating material molecules at very high velocities, in the order of 400÷1300 m/s, which due to the collision with the ground undergo high plasticization. It is enabled by dynamic reaction of burning liquid fuel or gaseous fuel (hydrogen, methane, kerosene) with oxygen, where the flame temperature reaches 2500÷3000 °C. The additional material in the form of a powder is fed by a transporting gas (usually nitrogen) directly into the accelerated flame. The combustion heat of the fuel causes a strong plasticization of the powder particles, but they do not become liquefied. Their residence time in the flame zone is very short, this is due to the very high flow velocity characteristic of the HVOF process. Despite the short flight time of molecules and the strong protective atmosphere, molecules oxidize, but the high kinetic energy of the stream during collision with the ground causes flattening of the particles and breaking of the surface oxide layer. Sometimes individual powder particles in the spray stream are so small that the entire volume is oxidized. During microscopic observations, oxide inclusions characteristic for this process can be noticed. Coatings obtained in the HVOF process are characterized by very low porosity [1÷4].

The diagram of the supersonic flame spraying process is shown in Figure 1.



Rys. 1. Schemat procesu natryskiwania płomieniowego HVOF [4]

The HVOF method can use a wide range of different coating materials (composites, non-ferrous metals, ceramics, transition metals). The quality and adhesion of the obtained coating depends on the type of additive material used, its chemical affinity with the substrate material and preparation of the substrate surface directly before spraying. In addition to the physico-chemical and metallurgical factors, technological process parameters are also important: powder output, fuel flow and transport gas velocities, nozzle distance from the sprayed substrate, powder granulation etc. Co-operation of high kinetic energy of the stream and appropriately prepared substrate surface causes mechanical

jamming of particles of the coating material in the substrate. Surface which is dry, degreased, free of oxides and impurities, and above all having a suitable roughness is considered as well-prepared. The surface profile should be irregular and inhomogeneous, and have a kind of „sockets” in which it will be possible to deposit striking molecules of plasticized material [5÷7].

The aim of this work is to develop a flame supersonic spraying technology of nickel-chromium powder with the addition of Rhenium (Ni-Cr-Re) on a 16Mo3 boiler steel substrate and coating characterization.

The Rhenium is a refractory dark silvery element from the group of transition metals with an atomic number of 75 and an atomic mass of 186.2. It is characterized by a very high melting temperature (3180 °C), the third highest after carbon and tungsten, and Young’s modulus – 470 GPa. It is characterized by the fourth of the largest densities (21.02 g/cm<sup>3</sup>), giving way to osmium, iridium and platinum. At the temperatures of 2700÷2800 °C and high stresses, the tensile strength and high temperature creep of rhenium significantly exceeds tungsten. Unique rhenium properties are used wherever extremely high temperature values are encountered. It is used in the aerospace and missile industries for the production of jet engine components, in the electrotechnical industry, on electrical contacts, where the temperature values are extremely high, or in the power industry. Addition of rhenium to Ni-Cr powder is supposed to increase the heat resistance of the obtained coating and to improve resistance to high temperature oxidation [9÷11].

## Materials and devices

The substrate material was 16Mo3 chromium-molybdenum boiler steel. It has been successfully used in the power industry for the construction of boilers, pipelines and pressure vessels. The chemical composition of this steel is shown in Table I. The coating was sprayed onto 100 x 50 x 4 mm boards.

Mechanical properties according to EN 10273:2007:

- yield strength  $R_{p0.2} > 275$  [MPa],
- tensile strength  $R_m = 440\div590$  [MPa],
- extension  $A > 24\%$
- yield strength at 500 °C,  $R_{p0.2} = 141$  [MPa],
- creep resistance at 500 °C,  $R_{z100000} = 90$  [MPa].

The base additive material was Oerlikon Amdry 4535 nickel-chromium powder enriched with 1% of pure metallic rhenium. The chemical composition of the powder is shown in Table II.

The morphology of the base powder without the addition of rhenium is shown in Figure 2. Fractions with spheroidal geometry can be observed, the diameter of which oscillates in the 20÷45 µm range.

The metallic rhenium powder was characterized by an irregular shape and varied particle sizes in the range of 2÷10 µm. The morphology of Re powder is shown in Figure 3.

The target coating material used for spraying arose as a result of high energy grinding in a ball mill of the previously described powders with a 1% weight of rhenium. Figure 4 shows the morphology of the obtained mixture. A backscattered ions detector which generates compositional contrast

**Table II.** Chemical composition of Oerlikon Amdry 4535 powder [8]

Ni [%]	Cr [%]	Si [%]	Fe [%]	Mn [%]	Inne (max) [%]
Base	19.5	0.75	0.25	0.25	0.4

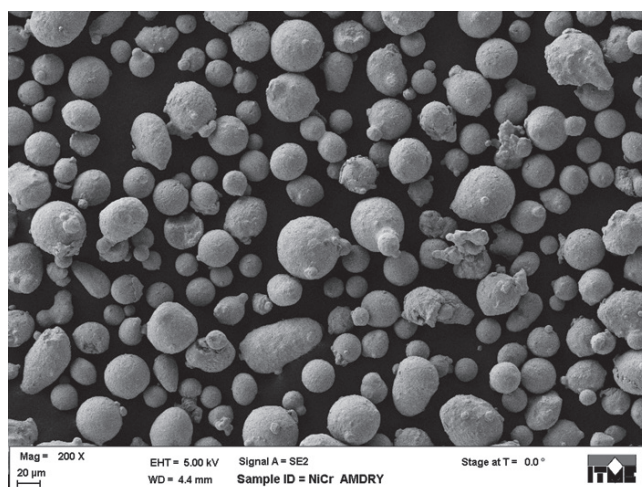


**Fig. 2.** Morphology of Oerlikon powder AMDRY 4535 (SEM)

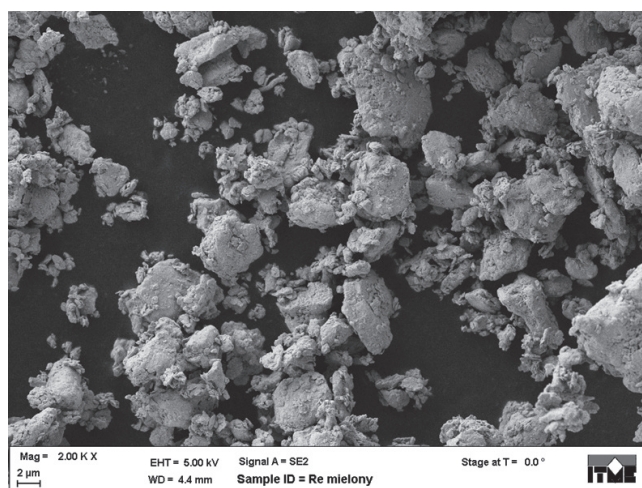


**Fig. 3.** Morphology of Re metallic powder (SEM)

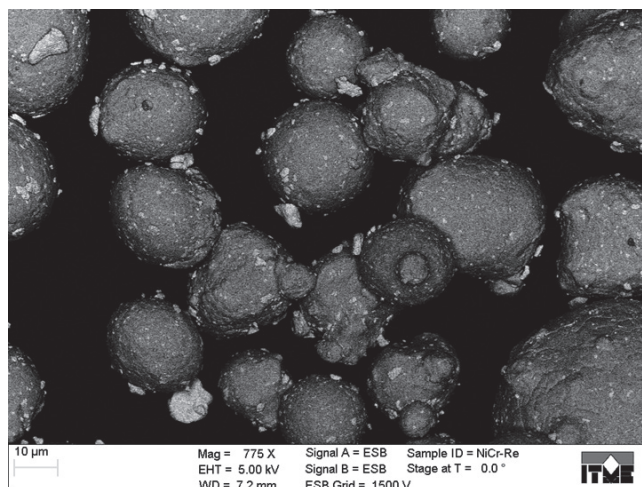


**Fig. 4.** Morphology of mixture of Ni-Cr-Re powder (SEM)

**Table I.** Chemical composition of 16Mo3 steel

According to Norm	Element content, % wt.										
	C	Si	Mn	P	S	Al	N	Cr	Cu	Mo	Ni
EN 10028-2:2009	0.12÷0.20	0.35	0.40÷0.90	0.025	0.010	–	0.012	0.30	0.30	0.25÷0.35	0.30

of materials with different atomic number was used. Re heavier than the nickel-chromium matrix gives a bright image that can be observed as lighter irregular fractions surrounding the nodular Ni-Cr molecules.

The spraying tests were carried out using the Flame Spray Technologies HV-50-JB device (Fig. 5), with water cooling of the burner (RESURS property, Czarodzieja 12, Warsaw).

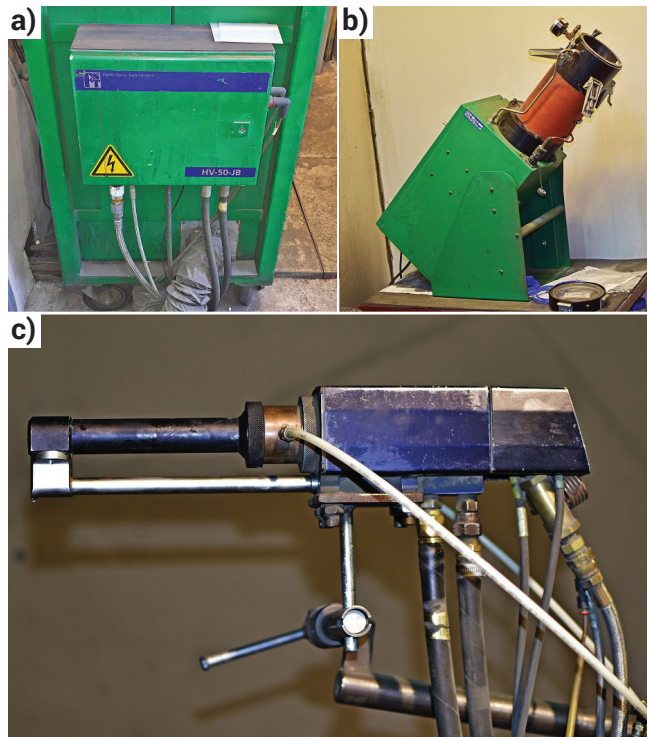


Fig. 5. HVOF-50-JB thermal spray device: a) feeding system, b) powder vessel, c) spray pistol JP5000 cooled with water

## The spraying process

Prior to the spraying process, the powder was dried at 300 °C for 60 h and sieved through a 50 µm screen, while the substrate was subjected to abrasive blasting using corundum. 10 pieces plates were attached to a steel holder for stable fixation during the process (Fig. 6). The high kinetic energy and pressure of the burner's stream can cause shifting of incorrectly set objects and, as a result, an uneven application of the coating.

Due to the width of the stream, one layer of the coating was planned for 4 passes of the burner to fully cover the width (50 mm) of the panels. The start of the process ran correctly, the parameters during the operation of the device were monitored on an ongoing basis. During the process, the temperature of the base material was monitored. After the sprayed substrate reached 130 °C, the process was stopped.



Fig. 6. The way of fixing the steel samples for spraying

After cooling to 30 °C, the subsequent layers were sprayed until the substrate material reached a temperature of 130 °C again. Cooling was supported by the air stream.

A total of 45 layers were applied until a coating thickness of approx. 650 µm was obtained.

Average values of parameters registered during all spraying attempts:

Expenditure of O<sub>2</sub>: 956 [l/min]

O<sub>2</sub> pressure: 12.5 [bar]

Expenditure of kerosene: 22 [l/h]

Kerosene pressure: 8.5 [bar]

Expenditure of N<sub>2</sub>: 15 [l/min]

Combustion pressure: 7.7 [bar]

Water flow: 23 [l/min]

Water pressure: 11 [bar]

Water temperature at the entrance to the burner: 12 [°C]

Water temperature at the exit from the burner: 32 [°C].

## Tests of the obtained coatings

Prior to destructive testing, non-contact surface roughness measurements were carried out. These tests were carried out on Optotom Sensofar S Neox optical profilometer. Roughness measurements of the coating and the steel substrate after abrasive blasting were made. The substrate's surface parameters are shown in Figure 7.

The average arithmetic deviation of the profile from the mean line Ra oscillates close to the value of 9÷10 µm. However, this is a parameter that does not give clear information about the profile run and the actual amplitude of the roughness height. An important parameter is the value of Rz, i.e. the average height of 10 extreme surface points (5 above the average line and 5 below the average line). Rz values of approx. 85 µm show a heterogeneous and irregular course of the profile and provide the aforementioned „sockets” in the surface to facilitate sealing of the coating molecules. To illustrate the course of the surface profile, a three-dimensional model was made (Fig. 8).

On the model we observe clear inequalities with high amplitude of height. The surface prepared in such a way favors the adhesion of the coating. The course of deviations from the medium line on the control measuring section was also generated (Fig. 9).

The height course on the control measuring section confirms the correctness of the Rz parameter measurement. Deviations from the middle line can be as high as 50 µm. For comparative purposes, measurements were also made of the surface profile of the coating after supersonic spraying. The set of coating's surface parameters is shown in Figure 10.

ISO 4287		
Amplitude parameters - Roughness profile		
Rp	57.9789 µm	Gaussian filter, 0.8 mm
Rv	25.9135 µm	Gaussian filter, 0.8 mm
Rz	83.8925 µm	Gaussian filter, 0.8 mm
Rc	55.8867 µm	Gaussian filter, 0.8 mm, ISO 4287 w/o ame...
Rt	86.3550 µm	Gaussian filter, 0.8 mm
Ra	9.29516 µm	Gaussian filter, 0.8 mm
Rq	12.2660 µm	Gaussian filter, 0.8 mm
Rsk	1.08806	Gaussian filter, 0.8 mm
Rku	3.97557	Gaussian filter, 0.8 mm
Material Ratio parameters - Roughness profile		
Rmr	0.136240 %	c = 1 µm under the highest peak, Gaussian...
Rdc	21.7154 µm	p = 20%, q = 80%, Gaussian filter, 0.8 mm

Fig. 7. Substrate's surface parameters after abrasive blasting

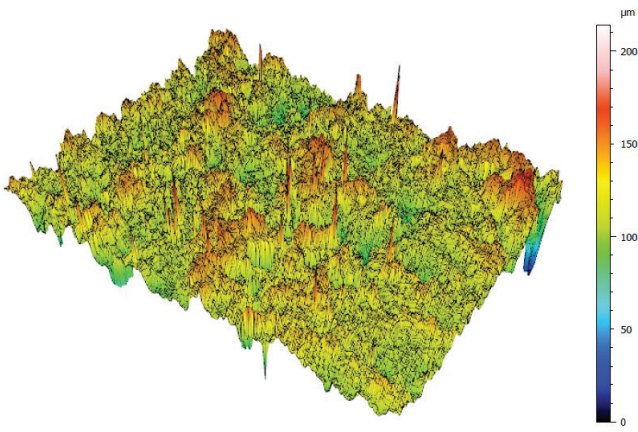


Fig. 8. Three-dimensional map of the substrate's surface

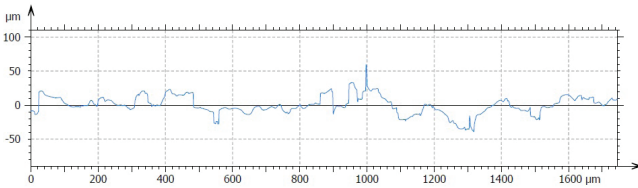


Fig. 9. Course of deviation from the medium line of the substrate after shot blasting

ISO 4287		
Amplitude parameters - Roughness profile		
Rp	13.9706 $\mu\text{m}$	Gaussian filter, 0.8 mm
Rv	21.7610 $\mu\text{m}$	Gaussian filter, 0.8 mm
Rz	35.7316 $\mu\text{m}$	Gaussian filter, 0.8 mm
Rc	19.1312 $\mu\text{m}$	Gaussian filter, 0.8 mm, ISO 4287 w/o ame...
Rt	35.7316 $\mu\text{m}$	Gaussian filter, 0.8 mm
Ra	7.30428 $\mu\text{m}$	Gaussian filter, 0.8 mm
Rq	8.48740 $\mu\text{m}$	Gaussian filter, 0.8 mm
Rsk	-0.234309	Gaussian filter, 0.8 mm
Rku	2.23084	Gaussian filter, 0.8 mm
Material Ratio parameters - Roughness profile		
Rmr	0.679348 %	$c = 1 \mu\text{m}$ under the highest peak, Gaussian...
Rdc	15.8702 $\mu\text{m}$	$p = 20\%$ , $q = 80\%$ , Gaussian filter, 0.8 mm

Fig. 10. Surface roughness parameters of the HVOF sprayed coating

The obtained coating is characterized by lower roughness than the substrate. The Ra parameter oscillates close to 7  $\mu\text{m}$ . The average height of 10 extreme points of the Rz surface, amounting to approx. 35  $\mu\text{m}$ , is more than twice lower than in the case of the surface of the substrate after abrasive blasting.

In comparison to the model of the substrate's surface, the amplitude of the height is clearly lower, the surface profile is more homogeneous (Fig. 11). There are no extreme elevations. The course of deviations from the medium line (Fig. 12) is also milder.

Figure 13 shows the macrostructure of the substrate-coating system. The substrate made of 16Mo3 steel with a ferritic-pearlitic structure is characterized by an even distribution of grains. A layer of oxide characteristic for the HVOF process was observed on the transition line (Fig. 14). The coating thickness is approx. 645  $\mu\text{m}$ .

Figure 15 shows the microstructure of the coating and substrate observed using a backscattered ions detector. The light-colored phase represents the distribution of Re particles in the coating, whose weight fraction constitutes approx. 1%.

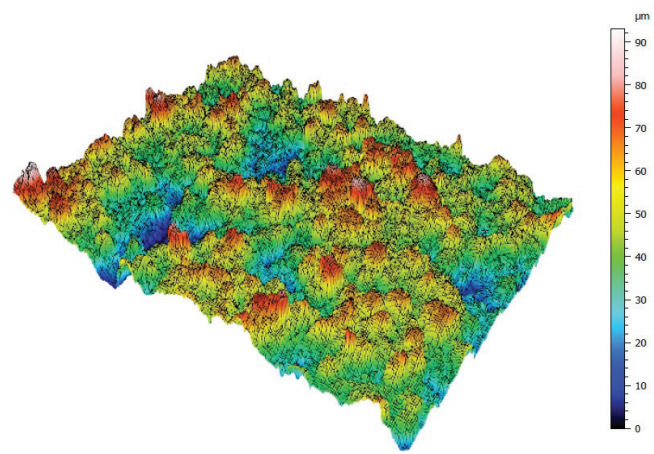


Fig. 11. Three-dimensional map of coating surface deposited by means HVOF spraying

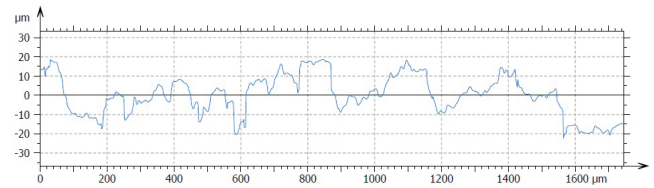


Fig. 12. Course of deviation from the medium line of the sprayed coating surface

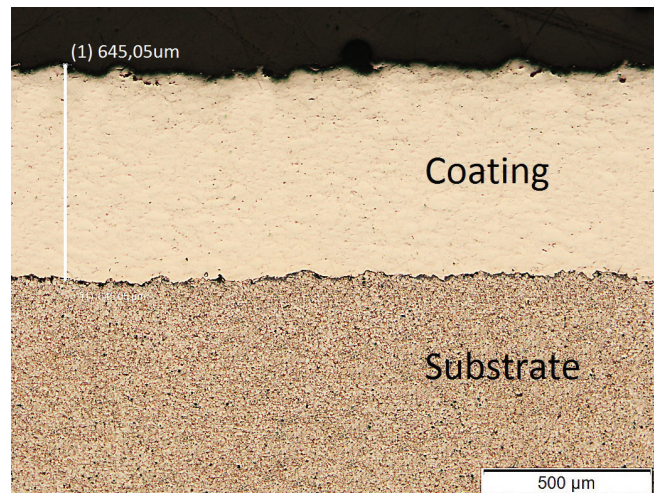


Fig. 13. Macrostructure of 16Mo3 steel substrate and Ni-Cr-Re coating

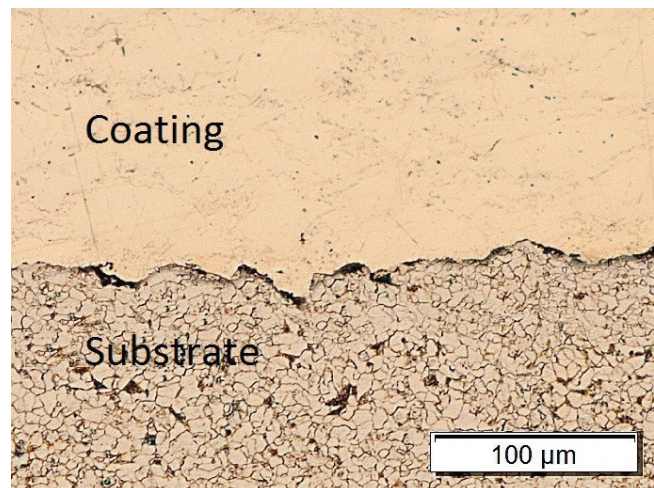


Fig. 14. Microstructure of 16Mo3 steel substrate and Ni-Cr-Re coating

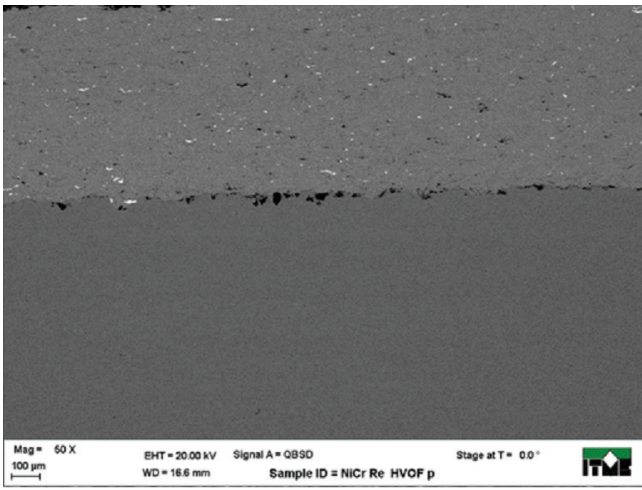


Fig. 15. Microstructure of substrate and Ni-Cr-Re coating (SEM)

The structure of the coating consists of highly deformed particles of the Ni-Cr matrix powder in which particles in the form of Re (Fig. 16) particles with dimensions of several micrometers are randomly dispersed.

In the next stage, the hardness of the coating was measured using the Vickers method according to PN-EN ISO 6507-1. The measurements were made under a 1 N load, and the results are shown in the graph (Fig. 17).

The graph shows the average value of the hardness of the five measurement series with the standard deviation for the measuring point at the confidence level of 95%. The measuring impulses were made with a 60 μm step. The hardness of the 16Mo3 steel substrate is approx. 180 HV0.1 with a relatively low standard deviation, which proves the homogeneity of the substrate material. The coating has a hardness in the range of 350÷400 HV0.1, with almost twice the value of the standard deviation from the average values. This confirms the heterogeneity and diversified structure of the coating.

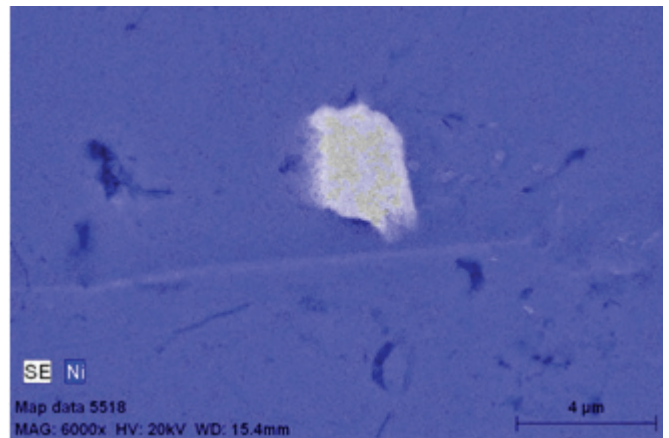
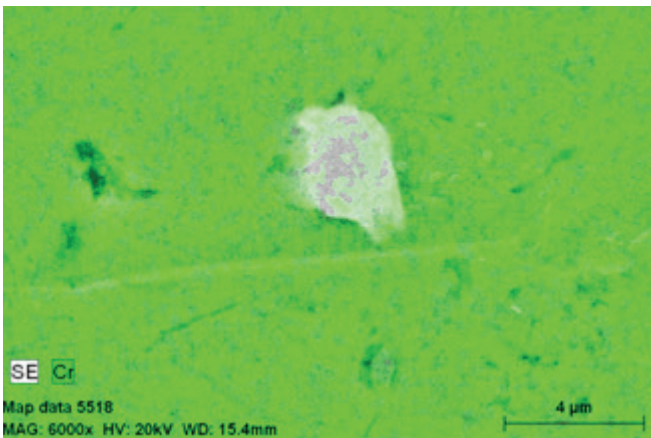
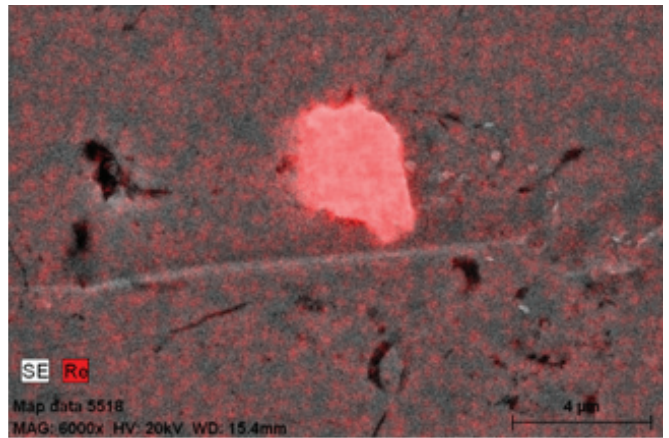
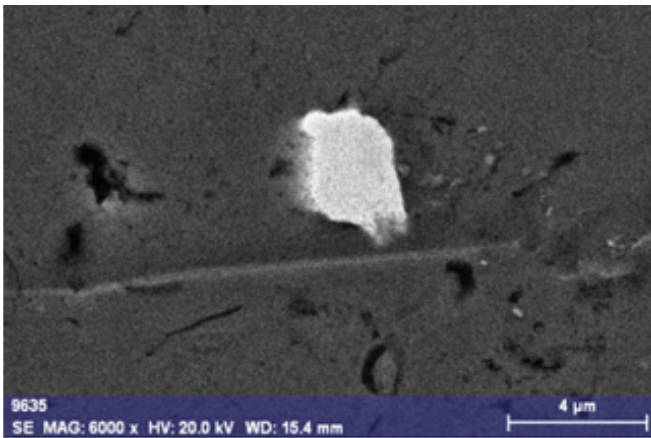


Fig. 16. Chemical analysis of SEM EDS area of the Re particle

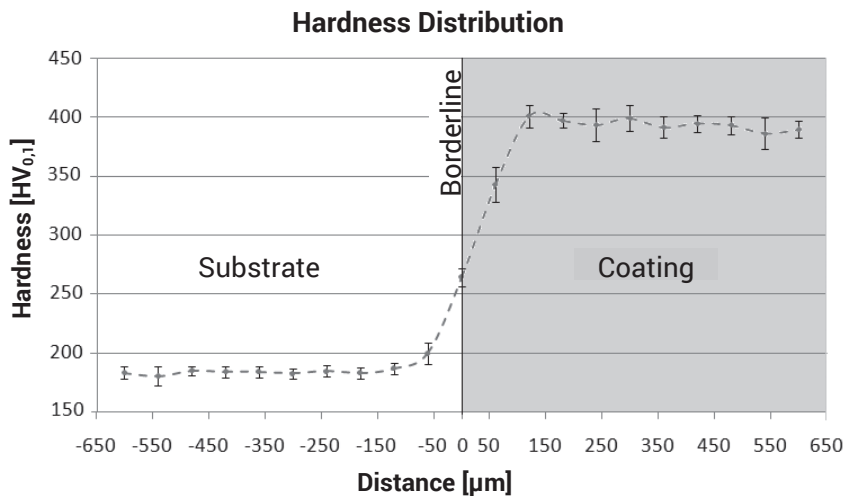


Fig. 17. Hardness distribution in substrate-coating system

## Summary and Conclusions

The HVOF supersonic flame spraying process offers a wide range of application possibilities. With appropriate selection of parameters, various metallic and composite additional materials can be used. Very few restrictions apply to the substrate, the condition is to prepare the surface to achieve maximum adhesion of the coating. Sprayed HVOF coatings are characterized by compact, dense packing of molecules and relatively low porosity. In many cases, it is a good alternative to conventional pad welding methods. In the metallurgical industry, this method is the foundation for the regeneration and preventive modification of the surface of machine parts. The nickel-based powder used is characterized by high corrosion and erosion resistance. The addition of rhenium increases the heat resistance of the alloy and resistance to oxidation when working at high temperature. The correct coatings were obtained with a continuous connection to the substrate. A shortcoming of the connection's structure are oxide layers on the transition line and between successive layers. Their formation is inevitable in the HVOF process, you can only try to limit their participation. The obtained Ni-Cr-Re coating is characterized by a relatively high hardness (twice as high as the hardness of the 16Mo3 steel substrate), reaching 400 HV0.1. This is due to the nature of the process, where highly plasticized particles bombard the substrate and strongly jam in unevenness. The structure of the coating reveals evenly dispersed Re particles with dimensions of several micrometers.

*Badania wykonano w ramach projektu „Innowacyjne powrocia Ni-Cr-Re o podwyższonej odporności korozyjnej i erozyjnej do zastosowań wysokotemperaturowych w przemyśle energetycznym” program M-ERA.NET Call 2016 nr umowy M-ERA.NET2/2016/01/2017*

*Autorzy artykułu składają serdeczne podziękowania Panu Andrzejowi Radziszewskiemu (RESURS ul. Czarodzieja 12, Warszawa) za udostępnienie stanowiska do natryskiwania naddźwiękowego oraz Panu Mariuszowi Włodowskiemu (OPTOTOM ul. Głębocka 54c, Warszawa) za pomoc w przeprowadzeniu badań chropowości powierzchni.*

## References

- [1] T. Chmielewski, D. Golański, Selected properties of Ti coatings deposited on ceramic AlN substrates by thermal spraying, *Welding International*, (2013), vol. 27 (8), 604-609, DOI:10.1080/09507116.2011.606146.
- [2] K. Ferenc, P. Cegielski, T. Chmielewski, *Technika Spawalnicza w Praktyce*, Poradnik inżyniera, konstruktora i spawacza, Verlag Dashofer (2009).
- [3] P. Siwek, T. Chmielewski, M. Chmielewski, Natryskiwanie łukowe powłok Fe-Al, *Welding Technology Review* (2018), vol. 90 (3), 62-67.
- [4] M. Niedzielska, T. Chmielewski, Warunki natryskiwania HVOF powłoki Cr3C2-NiCr na stal 316L, *Welding Technology Review* (2017), vol. 89 (3), 46-50.
- [5] W. Żórawski, N. Radek N, Mikrostruktura i właściwości natrykiwanych naddźwiękowo powłok WC-12Co po obróbce elektroiskrowej, *Welding Technology Review* (2012), vol. 84 (9), 46-50.
- [6] T. Chmielewski, Z. Sheng: Natryskiwanie powłok na bazie wybranych faz międzymetalicznych metodą High Efficiency Hypersonic Plasma Spraying, *Prace Naukowe Politechniki Warszawskiej. Mechanika* (2006), 49-58.
- [7] G. Y. Koga, W. Wolf, R. Schulz, S. Savole, C. Bolfarini, C.S. Kiminami, W.J. Botta, Corrosion and wear properties of FeCrMnCoSi HVOF coatings, *Surface and Coatings Technology* (2019), 357, 993-1003, DOI: 10.1016/j.surfcoat.2018.10.101.
- [8] <http://www.oerlikon.com>
- [9] S. Venetskii, Rhenium, *Metallurgist* (1971) vol. 15 (04), Russia.
- [10] V. Kindrachuk, N. Wanderka, J. Banhart, D. Mukherij, D. Del Genovese, J. Rosler, Effect of rhenium addition on the microstructure of the superalloy Inconel 706, *Acta Materialia* (2008), vol. 56 (7), 1609-1618, DOI:10.1016/j.actamat.2007.12.010.
- [11] L. Huang, X.F. Sun, H.R. Guan, Z.Q. Hu, Effect of rhenium addition on isothermal oxidation behavior of single-crystal Ni-based superalloy, *Surface and Coatings Technology* (2006), 200(24), 6863-6870, DOI:10.1016/j.surfcoat.2005.10.037.
- [12] K. Tobota, T. Chmielewski, Napawanie laserowe powłok ochronnych na powierzchniach roboczych łopatek turbin parowych, *Welding Technology Review* (2016), vol. 88 (12), 38-42.



© 2019 by the authors. Submitted for possible open access publication under the terms and conditions of the Creative Commons Attribution (CC BY) license (<http://creativecommons.org/licenses/by/4.0/>).